Supporting Information

Lu et al. 10.1073/pnas.1303687110

SI Materials and Methods

Plasmids. The full-length rat *Midline-1* (*Mid1*, GeneBank ID: 54252), *Mid1ΔCTD* (C terminus truncated form of Mid1) *Protein phosphatase 2A catalytic subunit* (*PP2Ac*, GeneBank ID: 19052), and *α4* (GeneBank ID: 18518) were cloned from rat brain cDNA and inserted into the pCAG-EGFP (CAG, chicken beta-actin promoter with CMV enhancer, modified from a commercial pCMV-EGFP vector) (Clontech) or pCAG-IRES-EGFP (IRES, internal ribosome entry site) expression vector. Mouse *Mid1* (GeneBank ID: 17318) was cloned from mouse brain cDNA and inserted into pEGFP-N1-3Flag. The human MID1-EGFP construct has been described previously (1). The RNAi sequences were inserted into pSUPER basic (Invitrogen) vector. The RNAi target sequence for mMid1 is GACTTGCGTTACTTGTGAA and for mPP2Ac is TTAAGAGCTACAAGCAGTGTA.

RNA Extraction and Real-Time PCR. Mouse (C57BL/6) forebrain tissues from embryonic or postnatal animals at different developmental stages (E14, E16, E18, P0, P3, P7, P14, and adult) were used for RNA extraction. Mice were killed via cervical dislocation, and brain tissues were quickly removed, dissected on ice, and homogenized with TRIzol Reagent (Invitrogen) at 4 °C. RNA was extracted according to the recommendations of the manufacturer, and the final RNA pellet was suspended in diethylpyrocarbonate (DEPC)-treated water, and 2 μg of total mRNA was further subjected to reverse transcription using oligo (dT) primers and Moloney murine leukemia virus (M-MLV) transcriptase (Invitrogen).

Real-time PCR was done with a LightCycler 480 Real-Time PCR System (Roche) according to the manufacturer's instructions. Starting RNA levels were quantified by using β-actin as the external standard. Primer sets were chosen from Primerbank, and gene sequences are available from the GenBank database. The primer sequences for the mouse *Mid1* gene (GeneBank ID: 17318) were as follows: forward, 5′-CTGTGACGGCACCTGTCTC-3′; reverse, 5′-AAACGGCTGACTGTTGGTCTT-3′; and β-actin (GeneBank ID: 11461): forward, 5′-GGCTGTATTCCCCTCCATCG-3′; reverse, 5′-CCAGTTGGTAACAATGCCATGT-3′. The primers were synthesized by Invitrogen.

In Situ Hybridization. In situ hybridization on the brain sections was performed with digoxigenin-labeled RNA probes. Full-length cDNA of Mid1 was amplified with specific PCR primers and cloned into pGEM-T easy vector (Promega) to generate an antisense probe for Mid1. The digoxigenin-labeled antisense probes were synthesized by in vitro transcription using SP6 RNA polymerase. Mice of different developmental stages were perfused with 4% (wt/vol) paraformaldehyde (PFA), and fixed brains were sectioned into 20-μm slices using a cryostat (μM). In situ hybridization was performed as described previously (2). Briefly, brain sections were hybridized for 18 h at 60 °C. The hybridization signal was detected with anti-digoxigenin–alkaline phosphatase Fab fragments (Roche) and nitro blue tetrazolium chloride (NBT) plus 5-bromo-4-chlor-indolyl-phosphate (BCIP) as color reaction substrates.

Neuron Culture and Transfection. Primary cortical neurons were prepared as previously described (3). In brief, the cortices or hippocampus of postnatal day 0 (P0) mice was dissected and digested with Trypsin (Sigma). Dissociated neurons were transfected using an AMAXA Nucleofector (Lonza) before plating following the modified protocol. Briefly, 200 μL of electroporation buffer was mixed with 3 μg of plasmid and ∼1 × 10^6 neurons for morphology analysis or with 20 μg of plasmid and ∼1 × 10^7 neurons for biochemistry assay. The cell/DNA suspension was then transferred into the cuvette, and the appropriate current was applied. Transfected neurons were plated onto coverslips or culture dish coated with poly-D-lysine (PDL). Medium was replaced 2–4 h later. Neuronal cultures were maintained in Neurobasal medium containing 2% (vol/vol) B27 (Gibco) in 5% (vol/vol) CO_2 at 37 °C. Neurons were fixed or harvested at 4 d in vitro (DIV).

Immunostaining and Image Acquisition. Cells were fixed and stained using different antibodies for image acquisition. Briefly, for neuronal morphology analysis, neurons were fixed at 4 DIV with 4% PFA plus 4% (wt/vol) sucrose and washed with 0.01 M PBS three times for 15 min in each, then permeabilized and blocked at room temperature for 1 h in blocking solution containing 5% (wt/vol) BSA and 0.1% Triton X-100. Subsequently, cells were incubated with different primary antibodies (Mid1, 1:100, Abcam; GFP, 1:1,000, Molecular Probes; Tau1, 1:1,000, Millipore; MAP2, 1:1,000, Neuromics; Tuj-1, 1:1,000, Neuromics; PP2Ac, 1:50, Cell Signal; acetylated-tubulin, 1:5,000, Sigma; tyrosinated-tubulin, 1:5,000, Abcam) diluted in blocking solution overnight at 4 °C. After washing with PBS (three times, 15 min each), cells were incubated with conjugated secondary antibodies (Molecular Probes) diluted in blocking solution at room termperature for 2 h.

For brain slices, immunostaining was performed using a free-floating protocol. Briefly, brain sections were incubated overnight with primary antibody (GFP, 1:1,000, Molecular Probes; Cux1, 1:500, Santa Cruz; Ctip2, 1:500, Abcam; Tbr1, 1:300, Abcam; Satb2, 1:200, Abcam) at 4 °C, washed three times in PBS, and then incubated with secondary antibody (1:2,000; Molecular Probes) for 2 h at room temperature, washed again in PBS, and incubated with Hoechst 33258 (Sigma) to clearly identify cortical layers and the morphological features defining S1 and S2.

Images were acquired by using a Nikon Neurolucida system or a ZEISS LSM 510 META confocal system.

Co-IP and Immunoblotting. For coimmunoprecipitation (co-IP), HEK293 cells or cultured cortical neurons were harvested with cold lysis buffer [50 mM Tris (pH 7.5), 150 mM NaCl, 1% Triton, 1 mM EGTA, 1 mM EDTA] with protease inhibitors, and IP was performed as described previously (4). Briefly, cell lysate was immunoprecipitated with different antibodies at 4 °C for more than 1 h and incubated with protein A or protein G-Agarose (20 μL; Roche) overnight at 4 °C.

Immunoprecipitates were collected and aspirated. The beads were resuspended in lysis buffer, washed at least five times, and incubated in SDS sample buffer for 5 min at 100 °C. The supernatant was subjected to immunoblotting.

Protein samples from cell lines, cultured neurons, and mouse brains were denatured and subjected to 9% (wt/vol) SDS/PAGE, transferred, and probed with antibodies against Mid1 (1:500; Abcam), PP2Ac (1:2,000; Cell Signaling), GAPDH (1:8,000; KangChen Biotechnology), and FLAG (1:2,000; Abmart) and visualized with enhanced chemiluminescence.

In Utero Electroporation. In utero electroporation was performed as described previously (5) with a few modifications. Briefly, E15 mice were anesthetized with sodium pentobarbital and subjected to abdominal incision to expose the uterus. For different ex-

periments, a mixture of GFP, RNAi, and/or overexpression constructs was prepared. Plasmids (about 1 μL) with 0.05% Fast Green (Sigma) were injected into the lateral ventricle through a glass micropipette. Electrical pulses were then delivered to embryos by gently clasping their heads with forcep-shaped electrodes connected to an ECM-830 square-pulse generator (BTX). Five 30-V pulses of 50 ms were applied at 1-s intervals. Uterine horns were repositioned in the abdominal cavity, and the abdominal wall and the skin were sutured. Postsurgery animals were maintained in a warm animal room (25 °C) with plenty of water and food supply. At different developmental stages, mice were perfused transcardially with 0.9% saline followed by 4% PFA in 0.1 M phosphate buffer (PB; pH 7.4), and the brains were removed and fixed in 4% PFA for another 24 h. Fixed brains were cryoprotected with 30% sucrose and then sectioned using a cryostat.

Axon Distribution Index Calculation. Brain slices (Bregma −1.58 mm) from P14 mice were stained with Hoechst and GFP. Both the GFP and Hoechst staining were imaged. The S1 and S2 areas were identified on the image of Hoechst staining, and the equivalent regions in GFP image were identified. Then the area and average GFP fluorescence intensity of S1 and S2 in both electroporated cell bodies (left hemisphere, L) and the contralateral hemisphere (right hemisphere, R) were measured with ImageJ. After subtracting the average fluorescence intensity of an unlabeled region from the fluorescence intensity of S1 or S2, the total fluorescence intensity (RFI) of each region was calculated as the fluorescence intensity multiplied by the area. The axon distribution index (ADI) is defined as $ADI = R_R/R_L = (RFI_{S2(R)}/RFI_{S1BF(R)})/(RFI_{S2(L)}/RFI_{S1BF(L)})$.

BrdU Labeling. For bromodeoxyuridine (BrdU) incorporation, E16 mice were intraperitoneally injected with 50 mg/kg BrdU (Sigma) and killed 2 h later. The brains were fixed in 4% PFA for 48 h and sectioned with a cryostat. For immunostaining, the brain slices were pretreated with 2 M HCl for 30 min at 37 °C to denature DNA and then neutralized in 0.1 M borate buffer (pH 8.5). The sections were then incubated with antibody against BrdU (1:1,000; Sigma) and washed with 0.01 M PBS.

Tractography. The 3D diffusion-weighted spin-echo images were acquired as previously described (6, 7) using a 16.4 Tesla vertical bore, small animal MRI system (Bruker Biospin; ParaVision v5.0) and a 15-mm linear, surface acoustic wave coil (M2M) at $0.1 \times 0.1 \times 0.1$ mm (uninterpolated) resolution. Each dataset was composed of two b0 values (b value of 0 and 5,000 s/mm^2, d/D = 2.5/14 ms) and 30 DW images.

Tractography was performed as previously described (7) using TrackVis (v0.4.4; www.trackvis.org) and Diffusion Toolkit, with HARDI/Qball modeling (8, 9) and a modified version of fiber assignment by continuous tracking (10, 11).

Streamline number and voxel number were obtained from TrackVis and plotted using GraphPad Prism V.4. Statistical differences between genotypes were assessed using an unpaired t test, where $P < 0.05$ and $n = 3$.

Image Tracing and Statistical Analysis. Neuronal morphology was traced using the software Neurolucida (V9.0; MBF), and the analysis was performed using the software Neurolucida Explorer (V9.0; MBF). Sholl analysis, a quantitative analysis by counting the number of neurite intersections of concentric circles of gradually increased radius centered at the cell body, was performed with Neurolucida Explorer (V9.0; MBF). Statistical comparisons were performed using a one-way analysis of variance followed by Student t test.

Time-Lapse Imaging. The neurons were transfected by electroporation as descried above before plating and maintained in Neurobasal medium containing 2% B27 (Gibco) in 5% CO_2 at 37 °C for 48 h. The time-lapse images were taken at 2-min intervals for 180 min using the Nikon Ti microscope. During the experiment, the culture dish was placed in a chamber to maintain the temperature and CO_2 concentration.

Growth Cone Collapse Assay and Growth Cone Turning Assay. Cortical neurons cultured form P0 mouse cortex were electroporated with pSUPER or Mid1 RNAi plasmid together with GFP before plating. In the growth cone collapse assay, 2 DIV neurons were incubated in normal culture medium (Neurobasal medium containing 2% B27) containing BSA (1 μg/mL) or Slit2 (1 μg/mL; R&D). Live images were acquired with the Nikon Ti microscope (60× objective, NA 1.4) at 5-min intervals for 30 min. During the experiment, the culture dish was placed in a chamber maintained at 37 °C and 5% CO_2. The percentage of collapsed growth cones in this period was quantified.

The growth cone turning assay was performed in Leibovitz-15 (L15) medium (Invitrogen) on neurons after 3–4 DIV. A micropipette (with 1-μm opening) filled with BSA (10 μg/mL), netrin-1 (5 μg/mL; R&D), or Wnt5a (10 μg/mL; R&D) was placed at a 45° angle ∼100 μm from the growth cone. The guidance cue gradient was generated by pipetting the solution with 2-Hz pulses (3 psi, 20 ms) using a PM8000 programmable pressure injector (Warner Instruments). Phase images were acquired with the Nikon Ti microscope [60× objective, numerical aperture (NA) 1.4] at 5-min intervals for 60 min. During the assay, the cells were maintained at 37 °C. Only growth cones that extended more than 5 μm were used for analysis. The turning angles were measured with ImageJ. Turning angles were defined as the angle between the original direction of growth cone and a line connecting the original and final positions of the growth cone.

Sorting GFP-Positive Neurons from Electroporated Mice Brain. Mice were electroporated at E15 with pSUPER or Mid1 RNAi plasmid together with GFP. At P0, the cortices were dissected, and then the GFP-positive tissue was microdissected under a dissection microscope equipped for fluorescence. After digestion in Papain, the cells were suspended in PBS with 1% FBS and subjected to fluorescence activated cell sorting (FACS). The GFP-positive and GFP-negative cells were separated on a MoFlo-XDP (Backman-Coulter) (excitation at 488 nm, emission at 525 nm) and collected in Neurobasal medium containing 2% B27 and 10% FBS. Forty-five thousand to 50,000 cells were used for Western blot analysis.

Anterograde and Retrograde Tracing. The 2- to 3-mo-old WT and Mid1 KO mice were used for the tracing experiment. Animals were anesthetized with sodium pentobarbital (0.7%), and the animal's heads were fixed in a stereotaxic frame. The desired region of brain was exposed by drilling a hole in the skull and further removing the dura under a dissection microscope. Then, 50 mg/mL biotinylated dextran amines (BDA-10,000; Molecular Probes; for anterograde tracing) or 1 mg/mL cholera toxin B subunit (CTb; Molecular Probes; for retrograde tracing) were injected with a glass pipette using air pressure. To trace from S1, the injection site was anterior-posterior (AP), −1.58 mm (Bregma); medial-lateral (ML), 3 mm; dorsal-ventral (DV), 1.3 mm. To trace from S2, the injection site was AP: −1.58 mm; ML, 3.7 mm; DV, 2.5 mm. For each brain, about 0.5 μL of tracer was injected over 10 min, and the pipette was left in position for another 5 min to reduce leakage. After injection, the skin was sutured, and the animals were placed at 37 °C for recovery. Then, 6–7 d after surgery, the animals were perfused as described above, and the brains were sectioned into 50-μm slices using a cryostat.

PP2A Phosphatase Activity Assay. The activity of PP2A was measured with a commercial kit from Millipore (catalog no. 17–313) following the manufacture's instructions. The phosphatase activity was assessed by quantifying the amount of phosphate generated from dephosphorylation of the phosphopeptide (K-R-pT-I-R-R), which can react with Malachite Green and be quantified by measuring the absorbance at 660 nm with a microplate reader. For cultured neurons, the cells were scraped into phosphatase extraction buffer (20 mM imidazole-HCl, 2 mM EDTA, pH 7.0, 10 mg/mL aprotinin, 10 mg/mL leupeptin, 10 mg/mL antipain, 10 mg/mL soybean trypsin inhibitor, 1 mM benzamidine, and 1 mM PMSF) and sonicated. After centrifuge at 2,000 × *g* for 5 min, the supernatants were used for the phosphatase activity assay. For brain tissue, 25 mg of tissue from the somatosensory cortex was homogenized on ice in 1 mL of phosphatase extraction buffer, and the supernatants were collected after centrifugation at 2,000 × *g* for 5 min. To perform the phosphatase activity assay, 4 μg of PP2Ac antibody and 40 μL of Protein A agarose was added to 200 μL of supernatant, and the total volume was brought to 500 μL with Ser/Thr assay buffer (50 mM Tris·HCl, pH7.0, 100 mM $CaCl_2$). Then, the sample was kept at 4 °C with constant rocking for 2 h. After washing the beads three times with Ser/Thr assay buffer, 60 μL of phosphopeptide (750 μM) and 20 μL of Ser/Thr assay buffer was added. After incubating for 10 min at 30 °C, 20 μL of supernatant was used to react with the Malachite Green solution, and the absorbance at 660 nm was measured. Simultaneously, the standard curve was made by adding different amounts of phosphate to the Malachite Green solution and measuring the absorbance at 660 nm. Finally, the PP2A activity was determined by comparing the absorbance values of samples to the standard curve.

1. Cox TC, et al. (2000) New mutations in MID1 provide support for loss of function as the cause of X-linked Opitz syndrome. *Hum Mol Genet* 9(17):2553–2562.
2. Tan GH, et al. (2012) Neuregulin 1 represses limbic epileptogenesis through ErbB4 in parvalbumin-expressing interneurons. *Nat Neurosci* 15(2):258–266.
3. Dotti CG, Sullivan CA, Banker GA (1988) The establishment of polarity by hippocampal neurons in culture. *J Neurosci* 8(4):1454–1468.
4. Chen Q, et al. (2010) CDKL5, a protein associated with rett syndrome, regulates neuronal morphogenesis via Rac1 signaling. *J Neurosci* 30(38):12777–12786.
5. Saito T (2006) In vivo electroporation in the embryonic mouse central nervous system. *Nat Protoc* 1(3):1552–1558.
6. Jones DK (2008) Tractography gone wild: Probabilistic fibre tracking using the wild bootstrap with diffusion tensor MRI. *IEEE Trans Med Imaging* 27(9):1268–1274.
7. Moldrich RX, et al. (2010) Comparative mouse brain tractography of diffusion magnetic resonance imaging. *Neuroimage* 51(3):1027–1036.
8. Tuch DS (2004) Q-ball imaging. *Magn Reson Med* 52(6):1358–1372.
9. Hess CP, Mukherjee P, Han ET, Xu D, Vigneron DB (2006) Q-ball reconstruction of multimodal fiber orientations using the spherical harmonic basis. *Magn Reson Med* 56(1):104–117.
10. Mori S, Crain BJ, Chacko VP, van Zijl PC (1999) Three-dimensional tracking of axonal projections in the brain by magnetic resonance imaging. *Ann Neurol* 45(2):265–269.
11. Kreher BW, et al. (2005) Multitensor approach for analysis and tracking of complex fiber configurations. *Magn Reson Med* 54(5):1216–1225.

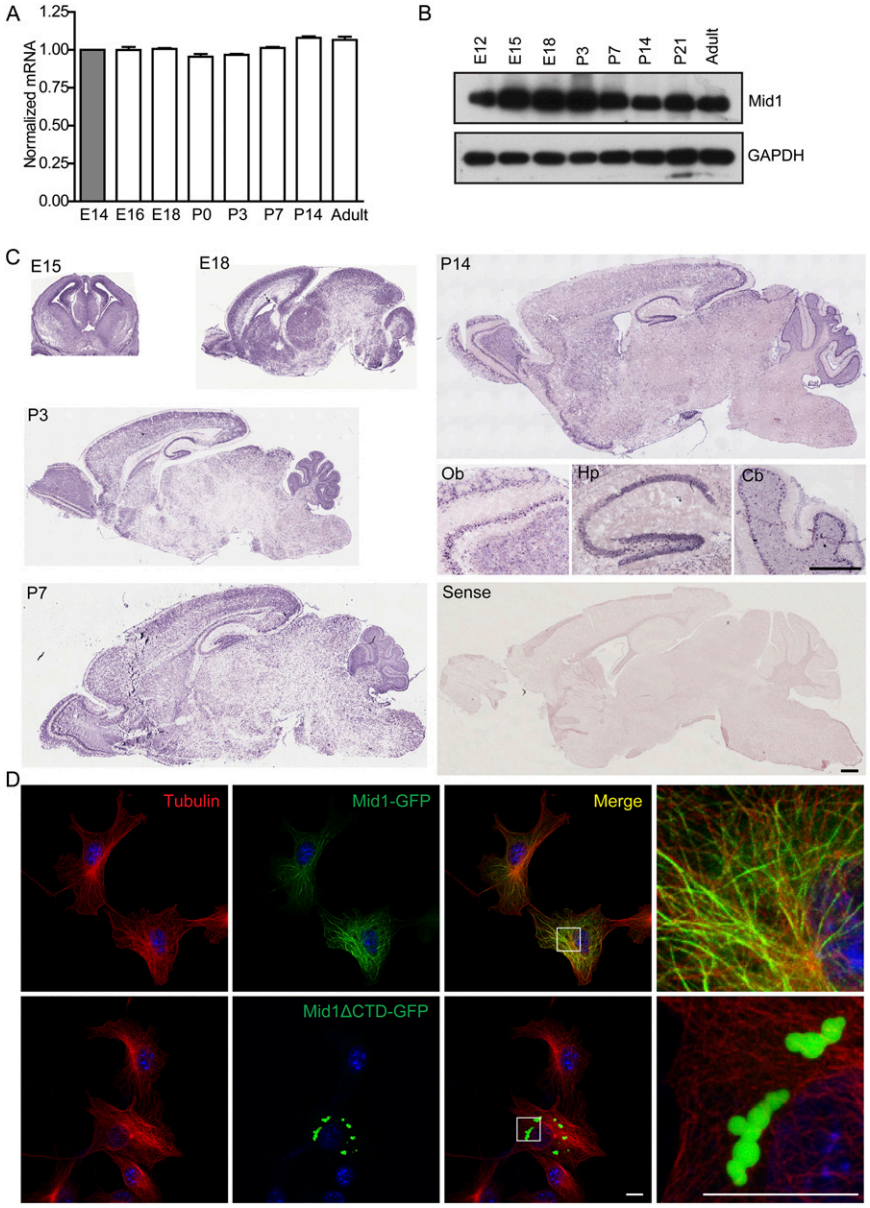

Fig. S1. Mid1 is expressed in the developing brain and is associated with microtubules. (*A*) Real-time, quantitative PCR analysis of the temporal expression pattern of *Mid1* mRNA in the cerebral cortex. The mRNA level of *β-actin* at each developmental stage was used as an internal control, and *Mid1* mRNA was normalized to *β-actin* at each time point; then, the ratios of *Mid1*/*β-actin* were further normalized to that at E14 for comparison. Results are shown as mean ± SEM, $n = 3$ at each stage. (*B*) Western blot analysis demonstrated that Mid1 protein was expressed in the cerebral cortex during development. Glyceraldehyde-3-phosphate dehydrogenase (GAPDH) was used as a loading control for comparison. (*C*) In situ hybridization of *Mid1* mRNA in a coronal section at E15, and in sagittal sections at E18, P3, P7, and P14 of mouse brains. Note that the Mid1 transcript is highly expressed in the ventricular zone at E15, and then within the cortical plate and in particular in the upper cortical layers from E18. At P14, Mid1 expression is higher in the occipital lobe of the cerebral cortex, as well as in the olfactory bulb (Ob), hippocampus (Hp), and cerebellum (Cb). A section labeled with the sense probe is shown as a negative control. (*D*) A Mid1 fusion protein, tagged with GFP, colocalizes with microtubules in COS7 cells. Immunostaining was performed against GFP and tubulin. The C terminus truncated form of Mid1 (Mid1ΔCTD-GFP) in not associated with microtubules and instead forms large aggregates in the cytoplasm. (Scale bars: *C*, 500 μm; *D*, 10 μm.)

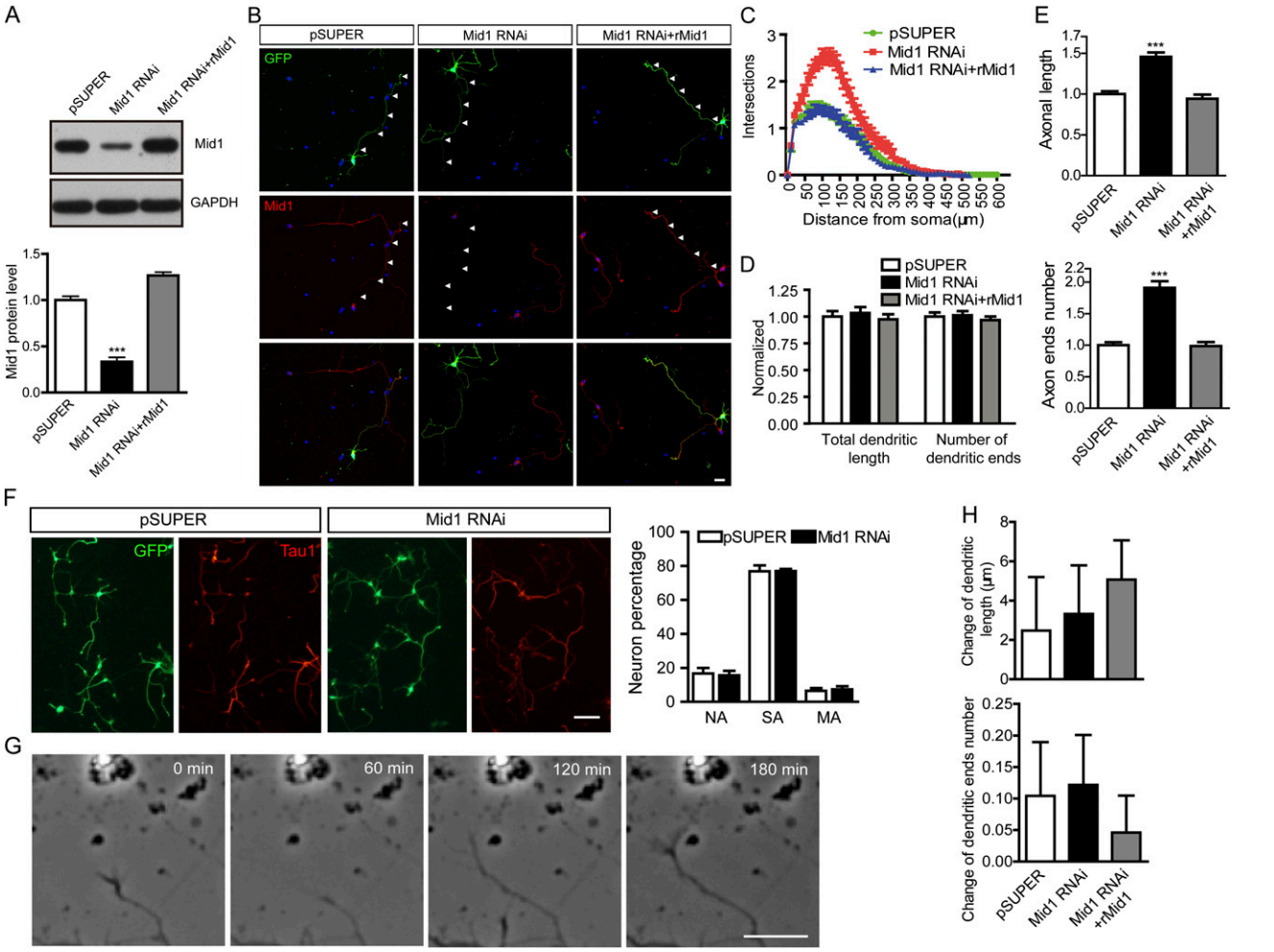

Fig. S2. Down-regulating Mid1 accelerates axonal growth but has little effect on the establishment of neuronal polarity. (*A*) To validate the Mid1 RNAi and rescue constructs, cortical neurons were transfected with pSUPER, Mid1 RNAi, or Mid1 RNAi plus rMid1 and subjected to Western blot analysis at 4 DIV. Quantitative analysis of the Mid1 protein level is shown in *Lower*. GAPDH was used as loading control. Results are from three independent experiments. ***$P <$ 0.001, Student *t* test. (*B*) Further validation of the Mid1 RNAi and rescue constructs was performed by immunostaining. Cultured cortical neurons transfected with the constructs indicated were stained with Mid1 antibody at 4 DIV. Arrowheads indicate the axons of transfected neurons. Note that the Mid1 immunostaining decreases specifically in Mid1 RNAi-transfected neurons. (*C*) Results of a quantitative Sholl analysis performed by counting the number of neurite intersections for concentric circles of gradually increased radius centered at the cell body. This analysis revealed that axonal complexity was increased in Mid1-depleted neurons. (*D*) Quantitative analysis of dendrite morphology in cultured neurons transfected with different constructs. More than 100 neurons from four independent experiments were analyzed in each group. Data are shown as mean ± SEM. (*E*) Knocking down of Mid1 in cultured hippocampal neurons leads to increased axonal length and axon ends number. About 100 neurons from three independent experiments were analyzed in each group. Data are shown as mean ± SEM, ***$P < 0.001$, *t* test. (*F*) Silencing Mid1 does not affect neuronal polarity. Cultured neurons were electroporated with indicated constructs at DIV0 and stained for GFP and axon marker Tau1 at 4 DIV. The percentages of cells with no axon (NA), single axon (SA), and multiple axons (MA) were calculated. Four independent experiments were performed. (*G*) High magnification view of the dashed boxed region in Fig. 2*C* at the indicated time points. (*H*) Quantification of neurite dynamics. The change of dendrite length and branch number in 180 min was measured and shown as mean ± SEM, $n = 48$ in the pSUPER group, $n = 74$ in the Mid1 RNAi group, and $n = 87$ in the Mid1 RNAi+rMid1 group. Data are shown as mean ± SEM. The statistical analysis shows that down-regulating Mid1 did not promote neurite growth in developing neurons. (Scale bars: *B* and *G*, 20 μm; *F*, 100 μm.)

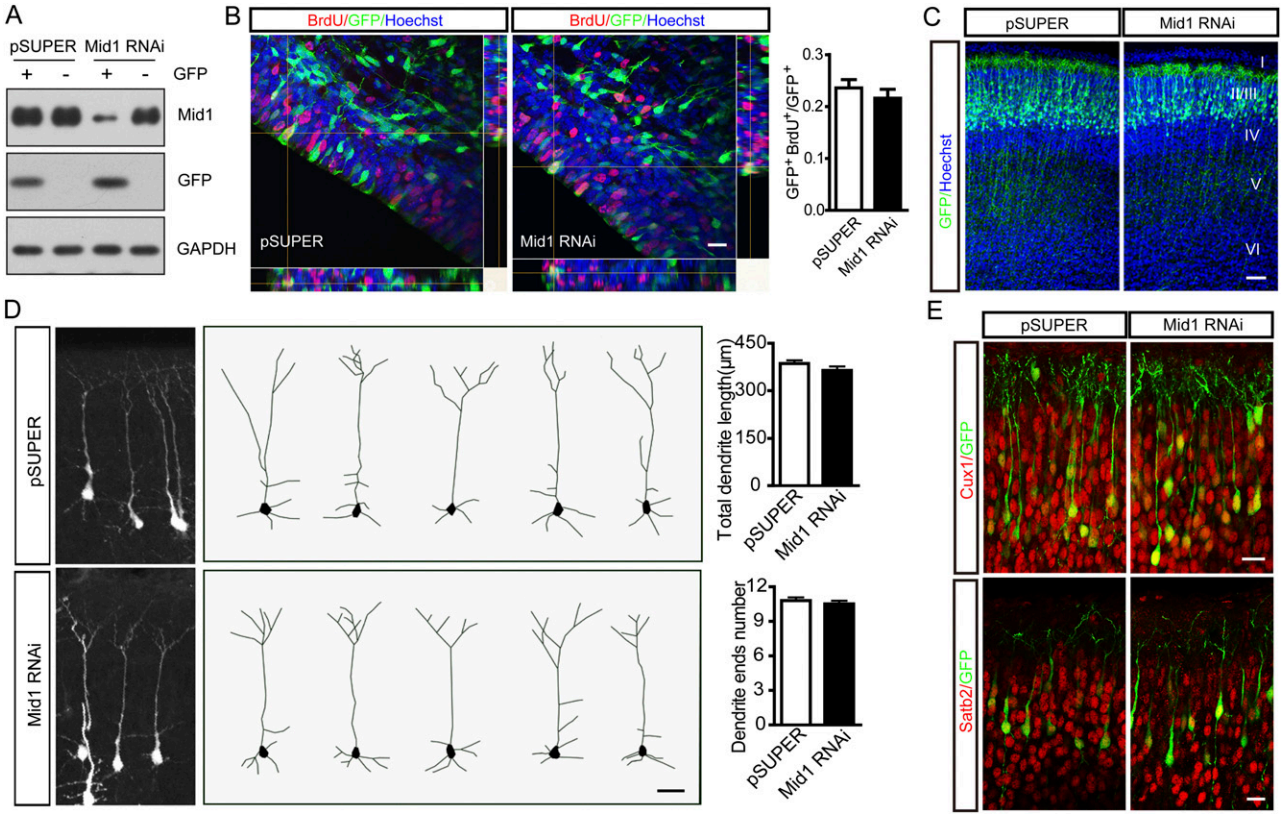

Fig. S3. Progenitor proliferation, neuronal migration, neuronal identity, and dendrite morphogenesis of Mid1-depleted cortical cells is not changed. GFP was coelectroporated with Mid1 RNAi or pSUPER construct into the paraventricular region of mice at E15. (*A*) Validating knockdown efficacy of Mid1 RNAi construct in vivo. Embryos were eletroporated with GFP together with either pSUPER or Mid1 RNAi construct at E15. At P0, cells in electroporated cortical regions were suspended and were separated through FACS. Both GFP-expressing cells and GFP-negative cells were further subjected to Western blotting. Note that Mid1 RNAi decreases the endogenous Mid1 protein in GFP-positive cells, compared with GFP-negative cells (nonelectroporated). (*B*) BrdU was injected at E16, and immunostaining against BrdU and GFP was performed. The percentage of GFP and BrdU double-positive cells in the total GFP-positive cells in VZ/SVZ was quantified. Eleven brain slices from four animals were analyzed in each group. (*C*) Neuronal migration is unaffected in Mid1-depleted neurons at P3. (*D*) Brain slices from P3 mice were stained with a GFP antibody, and individual layer III neurons were traced. Total dendritic length and number of dendritic ends were quantified. $n = 40$ in the pSUPER group and $n = 39$ in the Mid1 RNAi group. (*E*) Costaining of GFP and Cux1 and Satb2 of P3 brain slices. (Scale bars: *B*, *D*, and *E*, 20 μm; *C*, 80 μm.)

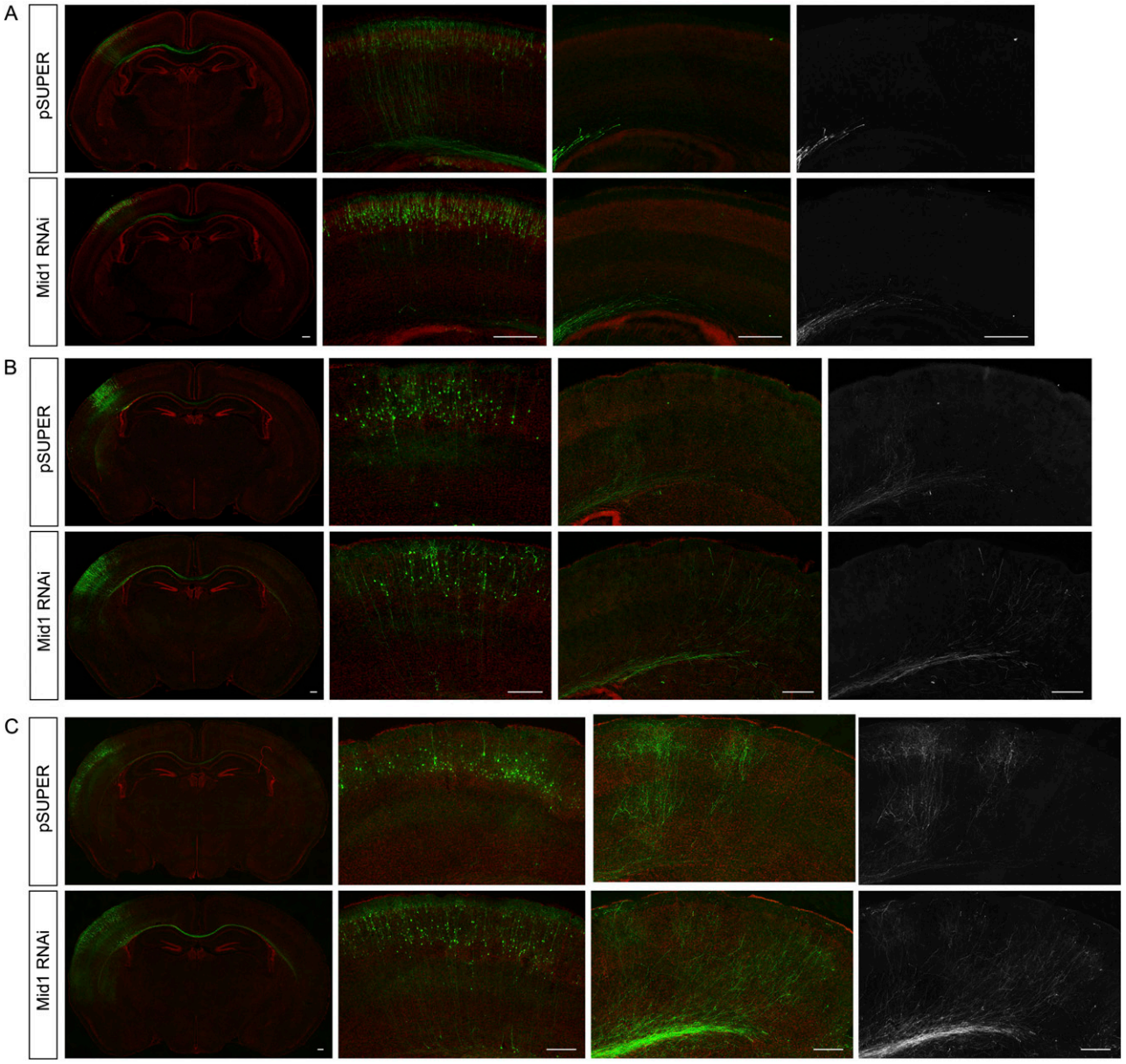

Fig. S4. Observing individual axon tips at different developmental stages with low quantity of GFP for in utero electroporation. In utero electroporation was performed at E15 as described previously. Instead of coelectroporating 1 μg/μL amount of GFP plasmid, we reduced the concentration of GFP plasmid to 0.1 μg/μL, for observing single axon tips in contralateral cortex. The first panel in each horizontal series of images is the entire view of the coronal sections to show the injection site and callosal axons crossing midline and projecting to the contralateral hemisphere. The injection site and projection area were further enlarged for observing individual neuronal cell bodies and the axon tips. The white and black images are identical to the enlarged images for each projection area after removing the red channel for better visualizing of individual axon tips. (*A*) In P4, both of the callosal axons from control and Mid1 RNAi group have crossed midline and were restrained within the corpus callosum. Few axon tips were seen penetrating into the cortical plate. However, the Mid1 RNAi axons show longer length. (*B*) In P7, single axon tips from control and Mid1 RNAi cells were seen in contralateral cortices. Callosal axons in control group started to project into the contralateral cortex at the S1/S2 border. In Mid1 RNAi animals, the majority of GFP-expressing axonal tips did not enter at S1/S2. Instead, they formed dispersed distribution throughout the S2 and Etc. (*C*) In P14, when control axons have already established a clear projection pattern in S1/S2, the Mid1 RNAi axons displayed a similar pattern with that of in P7 in contralateral cortex. (Scale bar, 200 μm.)

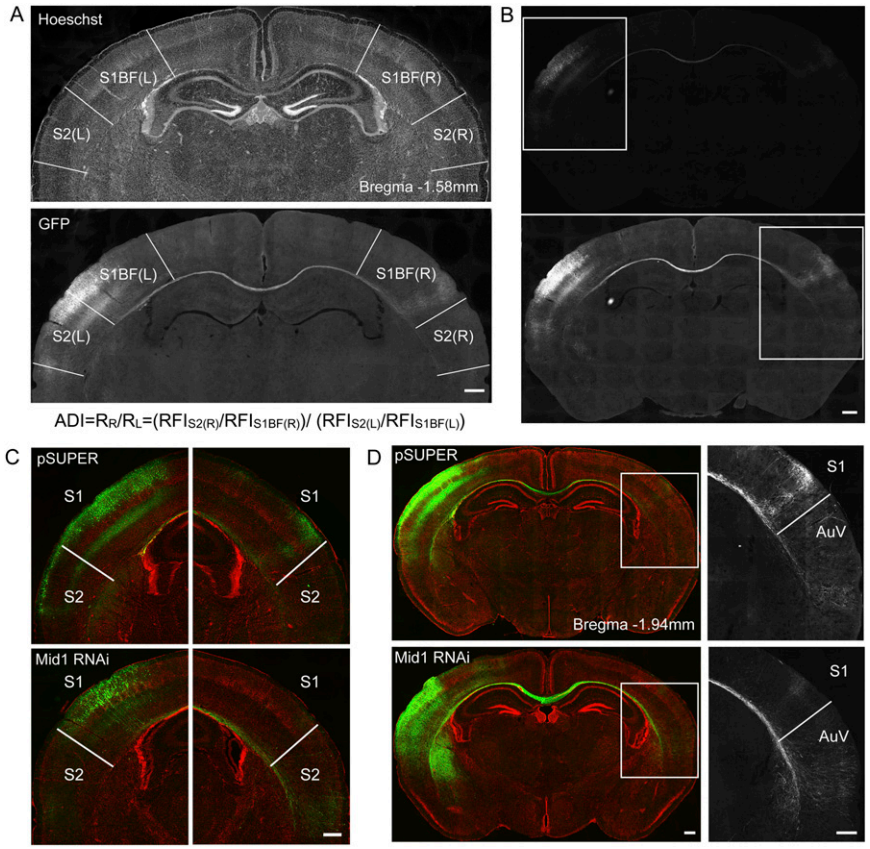

Fig. S5. (*A*) Illustration of the axon distribution index (ADI). GFP was transfected into the mouse brain at E15 and brain slices (Bregma −1.58 mm) from P14 mice were stained with Hoechst and GFP. The S1 and S2 regions are marked with white lines according to Hoechst staining. Relative fluorescence intensity (RFI) of these regions is measured and defined as RFI $_{S1BF(L)}$, RFI $_{S2(L)}$, RFI $_{S1BF(R)}$, and RFI $_{S2(R)}$. The ADI is defined as ADI = R_R/R_L = (RFI $_{S2(R)}$/RFI $_{S1BF(R)}$)/(RFI $_{S2(L)}$/RFI $_{S1BF(L)}$). To exclude the possibility that the differences between the ADI values could be caused by the inherent variability in both R_R and R_L, we chose brain slices (Bregma −1.58 mm) with similar electroporation efficacy and pattern on the electroporation side to keep the R_L values relatively constant. As a result, the ADI values were largely dependent on the value of R_R. (*B*) Example of different exposure time during image acquisition for proper visualization of cell bodies and axon terminals in each hemisphere. *Upper* shows that, when the optimal exposure time for electroporation site is selected, the axon terminals were too weak to see. *Lower* shows that, when the optimal exposure time for observing axon terminals is selected, the electroporation site became too bright to quantify. The boxed regions are shown in Fig. 3*C*, *Upper*. (*C*) Abnormal axonal projections are not eliminated during development. GFP and Hoechst staining of brain slices (Bregma −1.58 mm) from P30 mice show the projection pattern of transfected neurons. The mislocated axonal projections arising from Mid1-depleted cells were still present in the contralateral S2 region. (*D*) Staining of P14 coronal brain slices (Bregma −1.94 mm) with GFP antibody and Hoechst showed that the callosal axon terminals were mainly distributed in the S1 region, with a few terminals being observed in the AuV in pSUPER-transfected slices; however, in Mid1 RNAi-transfected brain slices, more axons grew beyond the S1 border and into the AuV region. (*Right*) A higher magnification view of the boxed regions of *Left*. AuV, secondary auditory cortex, ventral. (Scale bars: 500 μm.)

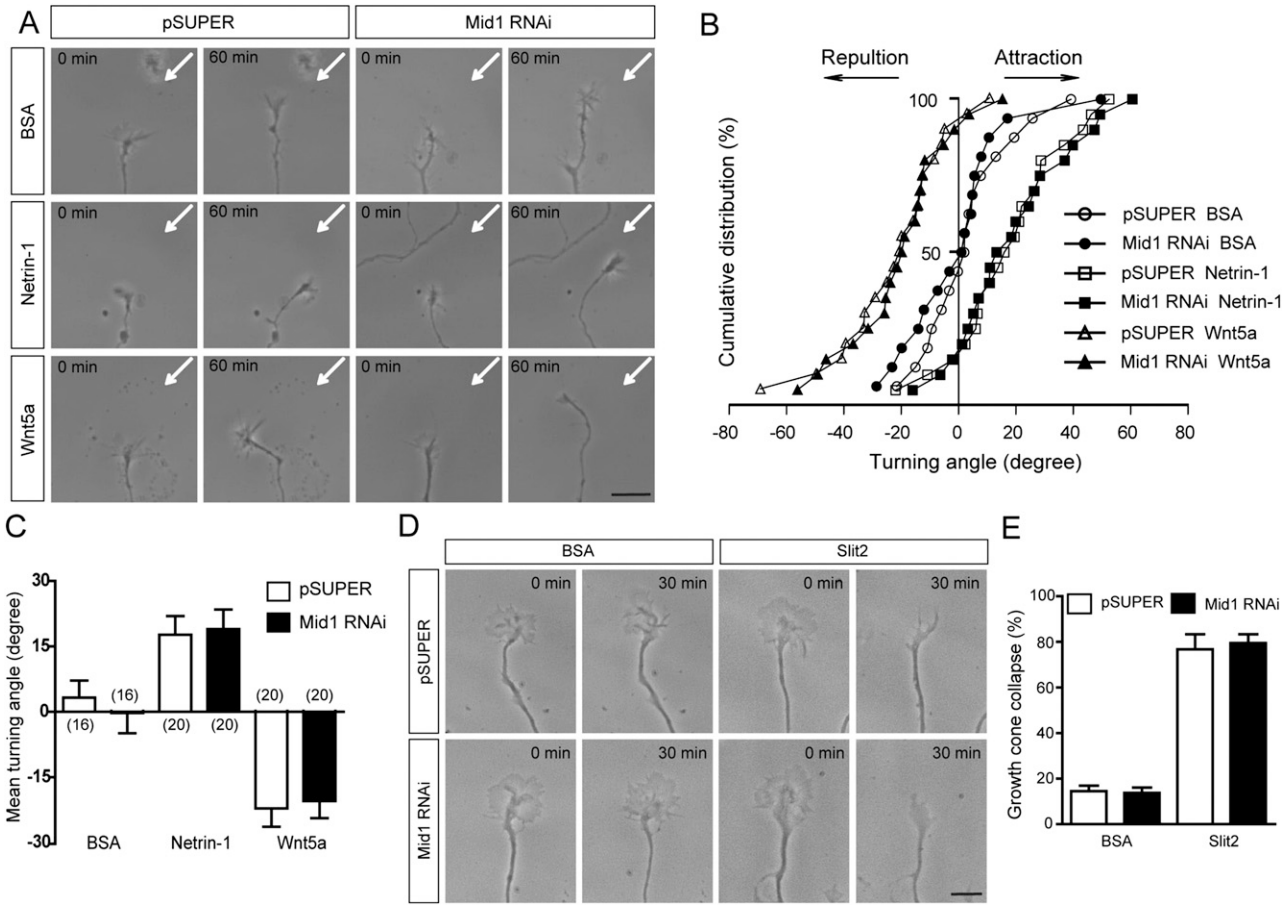

Fig. S6. Down-regulating Mid1 does not affect the response of axonal growth cone to Netrin-1, Wnt5a, and Slit2. (*A*–*C*) Cortical neurons were transfected with indicated constructs before plating, and a growth cone turning assay was performed at 3–4 DIV. (*A*) Representative axonal growth cones at the onset (0 min) and after 60 min onset of exposure to BSA, Netrin-1, or Wnt5a gradient. Arrows indicate the orientation of the gradient. (*B* and *C*) Cumulative distribution and mean turning angles of growth cones in different groups. Positive angle means attraction; negative angle means repulsion. The number of growth cones analyzed in each group was marked in *C*. (*D* and *E*) Cortical neurons were transfected with indicated constructs before plating, and a growth cone collapse assay was performed at 2 DIV. Representative growth cone images at the onset (0 min) and after 30 min onset of exposure to BSA or Slit2 were shown in *D*. The percentage of collapsed growth cones after 30 min administration of BSA or Slit2 were presented in *E*. The 70–80 growth cones from three independent experiments were analyzed in each group. (Scale bars: *A*, 10 μm; *D*, 5 μm.)

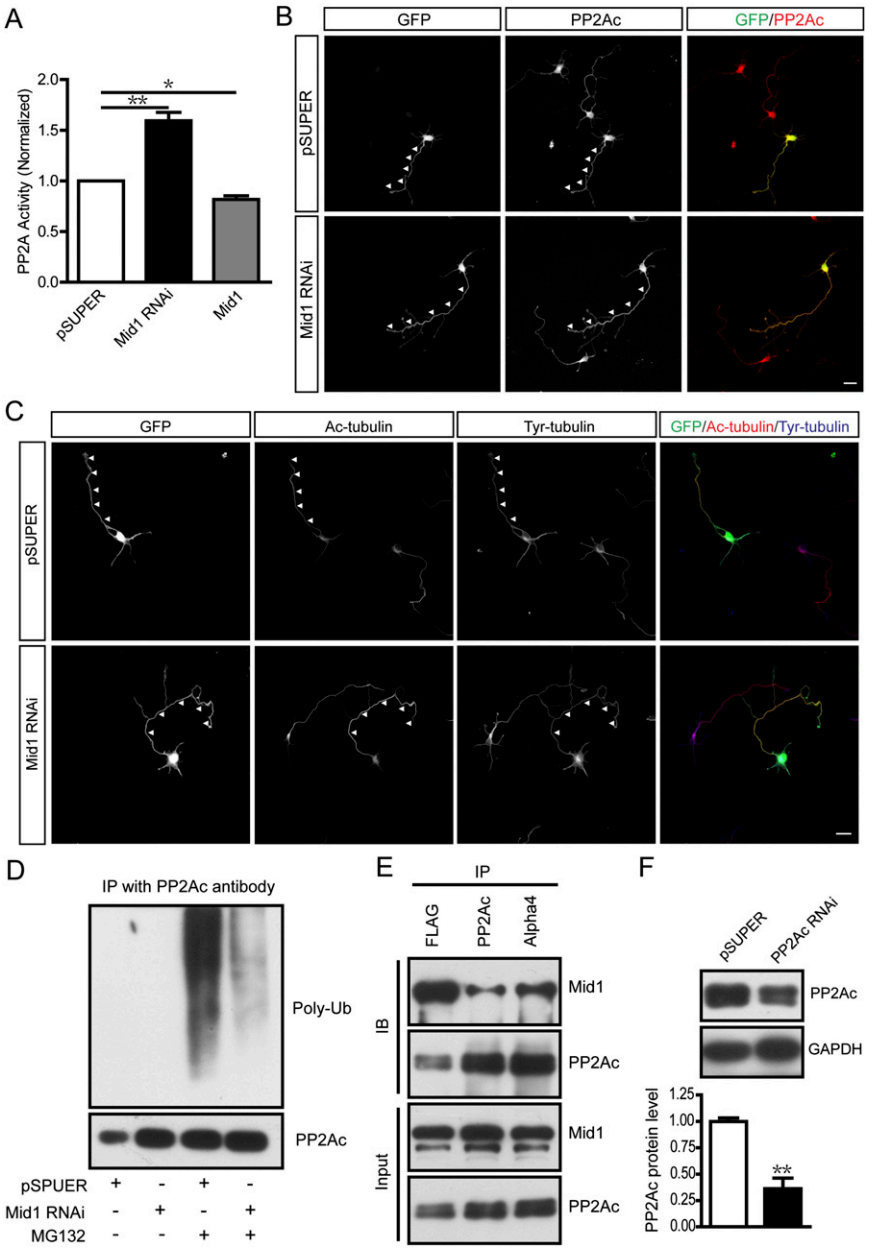

Fig. S7. Mid1 negatively regulates PP2Ac turnover. (*A*) Cortical neurons transfected with indicated constructs were harvested after 4 d in vitro (DIV), and the activity of PP2Ac in cell lysates was measured using a commercial kit. PP2Ac activity in pSUPER-transfected cells was defined as 1. $n = 5$ in each group, $^{*}P < 0.05$, $^{**}P < 0.01$, *t* test. (*B*) Cortical neurons transfected with indicated constructs were stained for PP2Ac at 3 DIV. The arrowheads indicate axon segments of neurons that were transfected with a control or Mid1 RNAi construct. Note that the PP2Ac intensity is increased in Mid1 RNAi neruons, compared with the adjacent nontransfected cell in the same field. (*C*) Three days in vitro cells were stained with both acetylated-tubulin (Ac-tubulin) and tyrosinated-tubulin (Tyr-tubulin). In the control group, the GFP-expressing cell showed similar intensity of Ac-tubulin and Tyr-tubulin with the nearby nontransfected cell. However, down-regulating Mid1 led to increased Ac-tubulin whereas the Tyr-tubulin remained unchanged, compared with the adjacent nontransfected cell. (*D*) Cortical neurons were transfected with pSUPER or Mid1 RNAi, and the cells were treated with DMSO or MG132 for 24 h. The protein level of PP2Ac was determined by Western blot. Immunoprecipitation was performed with PP2Ac antibody, and the ubiquitination level was detected with an antibody against polyubiquitin. (*E*) HEK293 cells were transfected with mouse Mid1 (with a FLAG tag), α4, and PP2Ac. Immunoprecipitation was performed with indicated antibodies. Mid1 and PP2Ac were detected with specific antibodies. (*F*) Validation of the efficiency of PP2Ac RNAi. Cultured neurons transfected with indicated constructs were subject to immunoblotting at 4 DIV. GAPDH was used as loading control in quantitative analysis. $n = 3$ in each group, $^{**}P < 0.01$, *t* test. (Scale bars: *B* and *C*, 20 μm.)

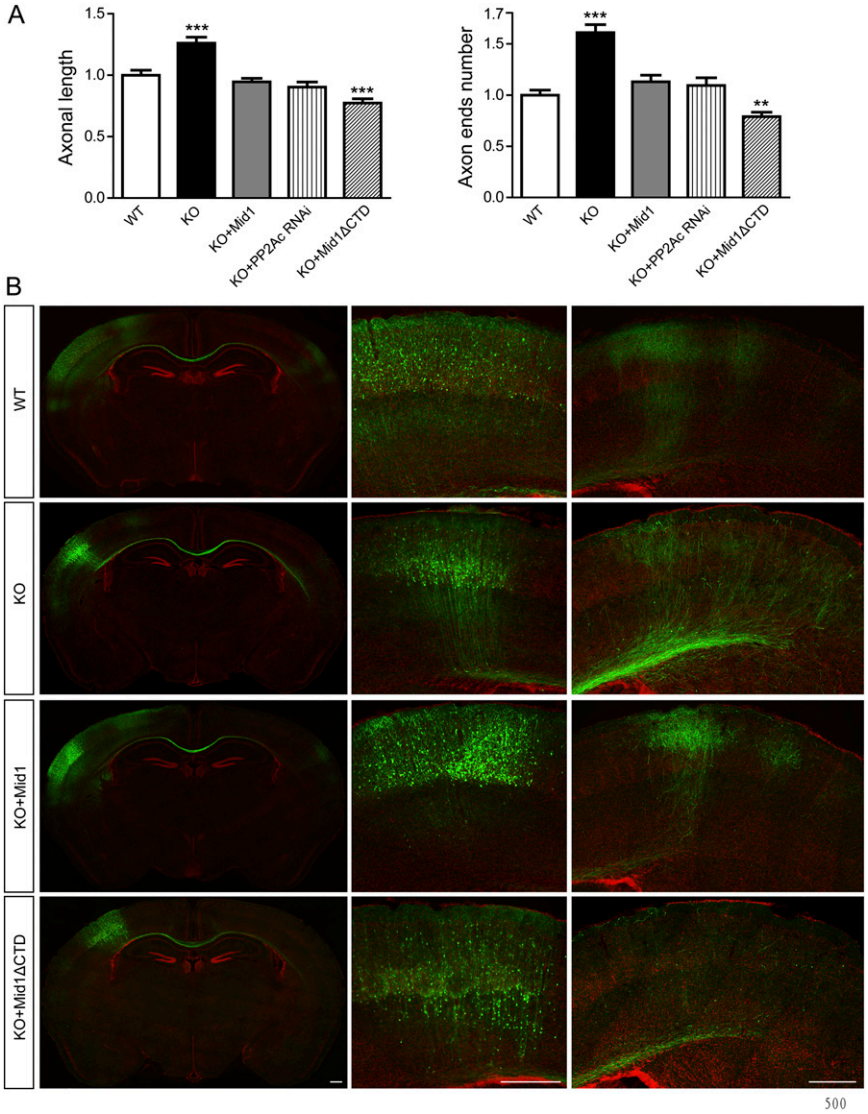

Fig. S8. Overexpressing Mid1ΔCTD decreased axonal length and branching number in cultured cortical neurons from *Mid1* KO animals. (*A*) In vitro study in *Mid1* KO cortical cultures. Cortical neurons from WT or *Mid1* KO mice were transfected with indicated constructs before plating. At 4 DIV, the neural morphology was analyzed. Then, 90–100 neurons from three independent experiments were analyzed in each group. Data are shown as mean ± SEM, $^{**}P < 0.01$, $^{***}P < 0.001$, *t* test. (*B*) Overexpressing Mid1ΔCTD in developing cortex in *Mid1* KOs affected radial migration and axon development. Mice were electroporated with indicated constructs at E15, and brain slices were collected from P14 animals. Note that a large number of cell bodies remained in lower cortical layers and that fewer axonal terminals are seen in the contralateral cortex. (Scale bar, 500 μm.)

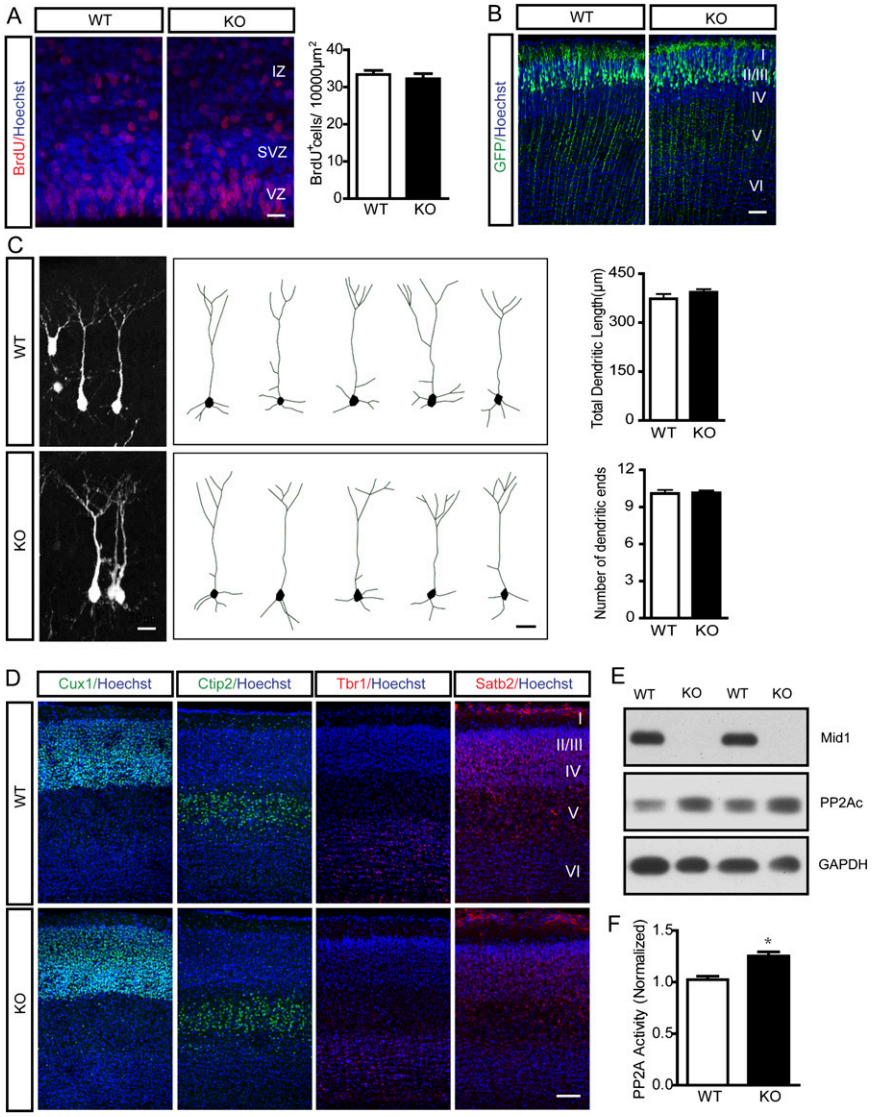

Fig. S9. Progenitor proliferation, neuronal migration, dendritic arborization, and cortical laminar structure are unperturbed in *Mid1* KO mice. (*A*) Quantification of the density of BrdU-positive cells in the VZ/SVZ of *Mid1* WT and KO mice at E16. $n = 6$ in the WT group and $n = 5$ in the KO group. (*B*) Neuronal migration is normal in *Mid1* KO mice at P3. (*C*) Dendrite outgrowth is not affected in *Mid* KO mice. Brain slices from P3 mice were stained for GFP, and individual neurons were traced. Quantitative analysis of total dendritic length and number of dendritic ends was performed. $n = 43$ in the WT group and $n = 40$ in the KO group. (*D*) The organization of cortical layers is normal in *Mid1* KO mice. Brain slices from P7 *Mid1* KO mice and their WT littermates were stained with antibodies against Cux1, Ctip2, Tbr1, and Satb2. Hoechst was stained to visualize the cortical layers. (*E*) Protein level of PP2Ac increases in *Mid1* KO mice. The somatosensory cortices of P14 *Mid1* WT and KO mice were isolated, and the protein levels of PP2Ac and Mid1 were determined by Western blot. GAPDH was used as loading control. (*F*) PP2Ac activity increases in *Mid1* KO mice. The somatosensory cortices of P14 WT and *Mid1* KO mice were isolated, and the activity of PP2Ac in tissue lysates was measured using a commercial kit. $n = 3$ in each group. $^*P < 0.05$, *t* test. (Scale bars: *A* and *C*, 20 μm; *B* and *D*, 80 μm.)

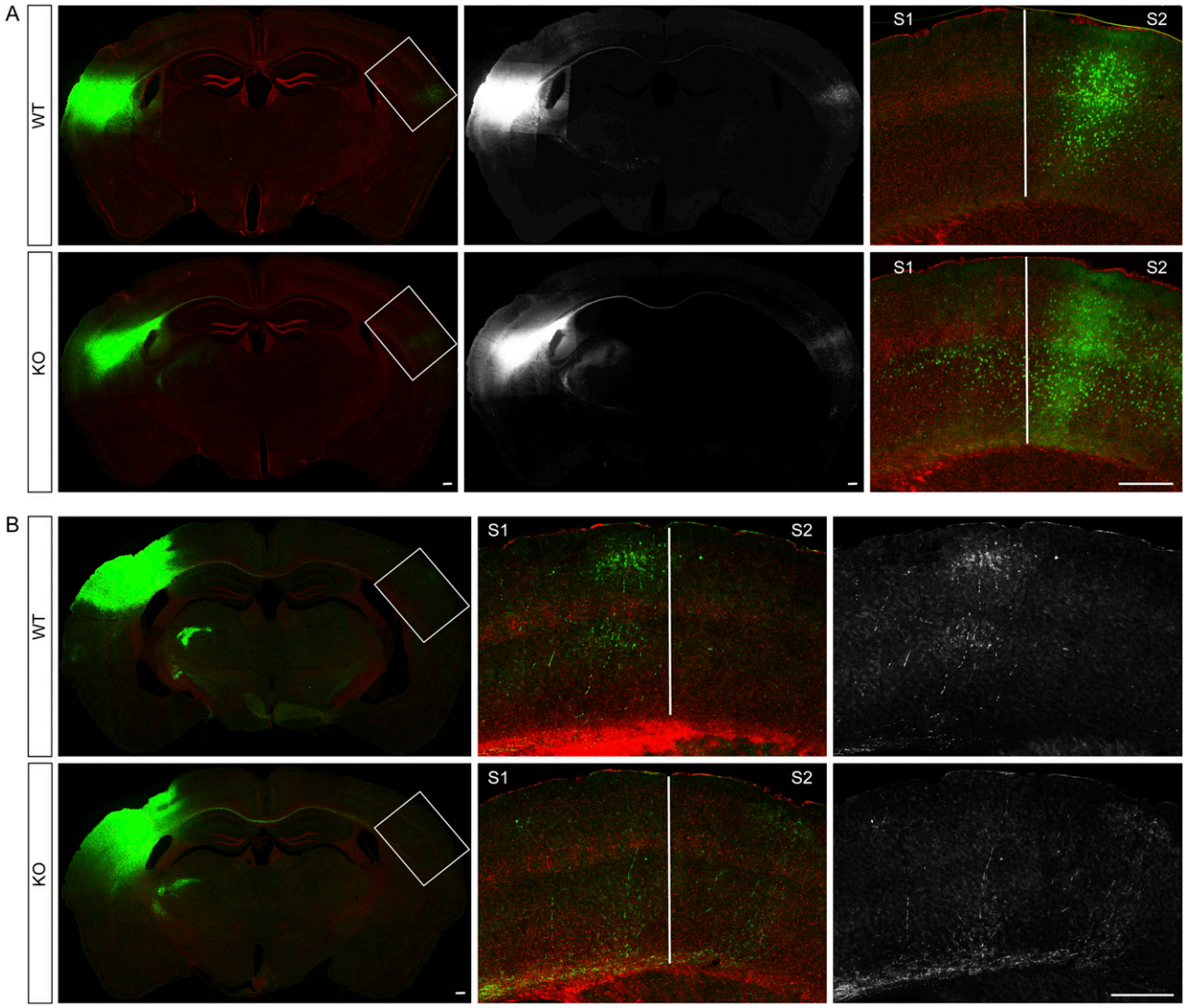

Fig. S10. Antero- and retrograde tracing of callosal axons. The anterograde tracer biotinylated dextran amines (BDA) or retrograde tracer cholera toxin b (CTb) was injected in the S1 or S2 region, respectively. The mice were killed 7 d later. Brain slices around Bregma −1.58 mm were imaged. (*Right*) High-magnification pictures showing the contralateral S1/S2 regions. (Scale bar: 500 μm.)